

## Charm quark mass dependence in the CTEQ NNLO global QCD analysis

---

**Jun Gao,<sup>a</sup> Marco Guzzi<sup>\*b</sup> and Pavel M. Nadolsky<sup>a</sup>**

<sup>a</sup>*Department of Physics, Southern Methodist University  
Dallas, TX 75275, USA*

<sup>b</sup>*Deutsches Elektronen-Synchrotron DESY  
Notkestrasse 85, 22607 Hamburg, Germany*

*E-mail: jung@mail.smu.edu, marco.guzzi@desy.de,  
nadolsky@physics.smu.edu*

We discuss the impact of the charm quark mass in the CTEQ NNLO global analysis of parton distribution functions of the proton. The  $\overline{\text{MS}}$  mass  $m_c(m_c)$  of the charm quark is extracted in the S-ACOT- $\chi$  heavy-quark factorization scheme at  $\mathcal{O}(\alpha_s^2)$  accuracy and found to be in agreement with the world-average value. Impact on  $m_c(m_c)$  of combined HERA-1 data on semiinclusive charm production at HERA collider and contributing systematic uncertainties are reviewed.

*XXI International Workshop on Deep-Inelastic Scattering and Related Subjects  
22-26 April, 2013  
Marseilles, France*

---

\*Speaker.

**Introduction.** Measurements of lepton-nucleon deep-inelastic scattering (DIS) cross sections become increasingly sensitive to scattering of heavy quarks,  $c$  and  $b$ , at energies comparable to heavy-quark masses. This progress motivated several recent analyses [1, 2, 3] to determine the mass  $m_c$  of the charm quark from the DIS and other hadronic data in fits of PDFs in the nucleon. The functional form of the PDFs preferred by the QCD data is dependent on the method by which heavy-quark masses are included in DIS structure functions [4]. Consequently various precision measurements at the LHC are dependent on the heavy-quark treatment in DIS experiments.

Combined cross sections on inclusive DIS and semiinclusive DIS charm production at the  $ep$  collider HERA [14, 2] have the best potential to constrain the charm mass. On the theory side, perturbative QCD (PQCD) calculations for neutral-current DIS exist at the 2-loop level in  $\alpha_s$  both for massless [5, 6, 7] and massive [8, 9, 10] quarks, while massless [11, 12] and some massive [13] coefficient functions were also obtained at the 3-loop level. With such accuracy, it is possible to determine the charm quark mass and its uncertainty from the DIS data. In Ref. [15] we explored constraints on the  $\overline{\text{MS}}$  charm mass  $m_c(m_c)$  in the CT10 NNLO PDF analysis in order to compare them to  $m_c$  determinations from non-DIS experiments and by other groups. This study examined the feasibility of the  $m_c$  extraction from DIS measurements, which are unique in their right as spacelike charm production processes. The other goal was to determine  $m_c(m_c)$  in a General Mass Variable Flavor Number (GM-VFN) scheme S-ACOT- $\chi$  [16], the default heavy-quark scheme of CT analyses. This scheme is well-suited for theoretical expolaration of factors affecting the determination of  $m_c(m_c)$ , as a result of its close connection to the QCD factorization theorem [18] for DIS with heavy quarks. Recently, the S-ACOT- $\chi$  calculations wer extended to  $\mathcal{O}(\alpha_s^2)$ , or NNLO, in NC DIS [17], which significantly reduced theoretical uncertainties compared to the previously employed [2] NLO S-ACOT calculations.

**Implementation of the  $\overline{\text{MS}}$  mass.** Our calculation [15] takes  $\overline{\text{MS}}$  quark masses as the input for the whole calculation. The transition from the 3-flavor to 4-flavor evolution in  $\alpha_s$  and PDFs occurs at the scale equal to this input mass. The massive 2-loop coefficient functions for neutral-current DIS with explicit creation of  $c\bar{c}$  pairs [9] and the operator matrix elements  $A_{ab}^{(k)}$  [19] that we use require the pole mass as their input. For these parts, the  $\overline{\text{MS}}$  mass is converted to the pole mass according to the 2-loop perturbative relation in Eq. (17) of [20]. The global fit is sensitive to the number of loops included in  $\overline{\text{MS}}$  conversion. We explore this sensitivity by implementing two methods. In the first method, the  $\overline{\text{MS}}$  mass is converted to the pole mass by the 2-loop relation in both  $\mathcal{O}(\alpha_s)$  and  $\mathcal{O}(\alpha_s^2)$  radiative contributions to heavy-quark coefficient functions. In the second method, the 2-loop (1-loop) conversion is performed in the  $\mathcal{O}(\alpha_s)$  and  $\mathcal{O}(\alpha_s^2)$  terms in the Wilson coefficient functions and OME's, respectively. This is argued to be equivalent to calculating DIS structure functions directly in terms of the  $\overline{\text{MS}}$  mass and improve perturbative convergence of the best-fit values for  $m_c(m_c)$  [21].

**Theoretical inputs.** Several aspects of the QCD calculation affect determination of  $m_c$ . In a comprehensive factorization scheme such as GM-VFN, the exact charm mass enters hard matrix elements for charm particle creation (FC) in the final state, such as  $\gamma^* g \rightarrow \bar{c}c$  in NC DIS. At the same time, GM-VFN introduces several energy scales that are *approximately* equal to the charm mass, including the switching scale between 3 and 4-active flavors and the effective mass in the flavor-excitation (FE) matrix elements (with incoming heavy quarks). Our analysis indicates that it is the exact  $m_c(m_c)$  in the FC cross sections, and not the approximate mass scales, that primarily

controls the agreement with the DIS data.

GM-VFN schemes used in the PDF fits [16, 24, 25, 26] differ primarily in the form of approximation for FE coefficient functions at  $Q$  comparable to  $m_c$ , due to powerlike contributions  $(m_c^2/Q^2)^p$  with  $p > 0$  arising near the threshold. In S-ACOT- $\chi$  the form of these contributions is selected based on the general consideration of energy-momentum conservation (reference 3 in [16]). Their detailed form can be varied to estimate the associated higher-order uncertainty in the extracted  $m_c$  by introducing a generalized rescaling variable  $\zeta$  [27], implicitly defined by  $x = \zeta \left(1 + \zeta^\lambda M_f^2/Q^2\right)^{-1}$ . The default (and best motivated) form of the rescaling variable is obtained assuming  $\lambda = 0$ . However, other values of  $\lambda$  between 0 and 1 can be used to estimate the uncertainty.

Theoretical systematic uncertainty	DIS scale	$\alpha_s(M_Z)$	$\lambda$	$\chi^2$ definition
Parameter range	$[Q/2, 2Q]$	$[0.116, 0.120]$	$[0, 0.2]$	–
$\delta m_c(m_c)$ (GeV)	+0.02 –0.02	+0.01 –0.01	+0.14 –0	+0.06 –0

**Table 1:** Shifts of the optimal value of the charm mass  $m_c(m_c)$  obtained by varying theoretical inputs.

Theoretical uncertainties are summarized in Table 1, showing shifts in the extracted  $m_c(m_c)$  due to the factorization/renormalization scale in DIS cross sections,  $\alpha_s(M_Z)$ , the  $\lambda$  parameter in the rescaling variable, and implementation of experimental correlated systematic errors. The last source of uncertainty arises from the existence of several prescriptions (designated as “extended T” and “D” methods in Ref. [28]) for including correlated systematic errors from the fitted experiments into the figure-of-merit function  $\chi^2$ .

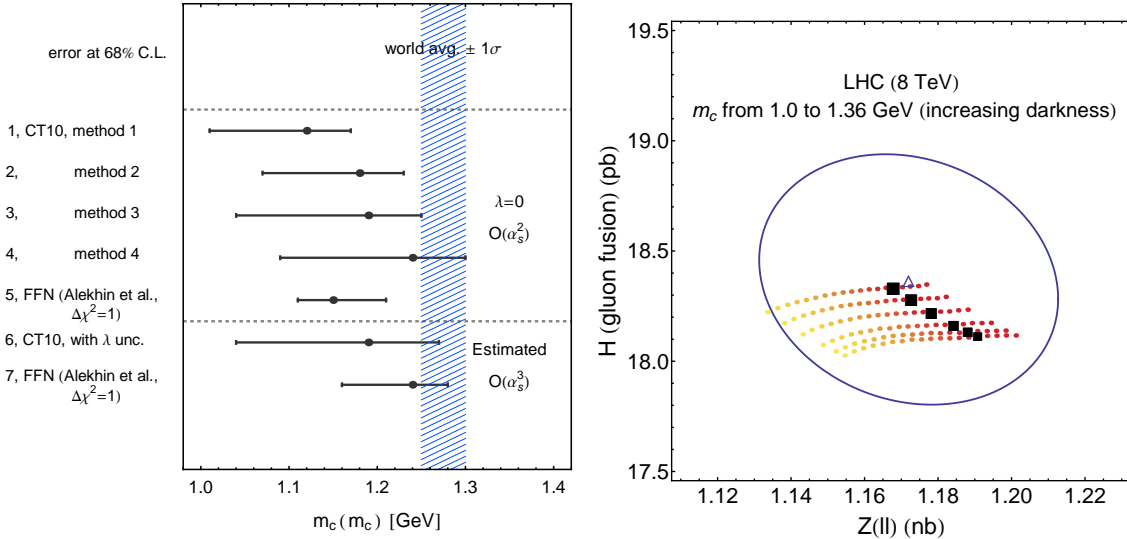


**Figure 1:** (a) Best-fit values of  $m_c(m_c)$  with uncertainties. (b) NNLO cross sections for SM  $H^0$  boson and  $Z^0$  boson production at the LHC 8 TeV.

**Results of the fit.** Our main results are illustrated in Fig. 1, with details provided in Ref.[15]. The left subfigure shows the best-fit  $m_c$  and its uncertainties. At order  $\alpha_s^2$ , the highest fully implemented order in our calculation, these values are found with four methods. Methods 1 and 2

correspond to the “extended  $T$ ” and “experimental”  $\chi^2$  definitions respectively [28], both using the full  $\overline{MS} \rightarrow$  pole mass conversion formula, and  $\lambda = 0$ . The best-fit values indicated by methods 3 and 4 correspond to the truncated mass conversion for the two  $\chi^2$  definitions previously mentioned. The resulting  $m_c(m_c)$  values in the four methods are  $1.12_{-0.11}^{+0.05}$ ,  $1.18_{-0.11}^{+0.05}$ ,  $1.19_{-0.15}^{+0.06}$  and  $1.24_{-0.15}^{+0.06}$  GeV, respectively. Here we quote the 68% C.L. PDF uncertainties defined as in the CT10 analysis [29] based on the value of the total  $\chi^2$  and agreement with individual experiments.

As we see, there is some spread in the  $m_c$  values depending on the adopted  $\overline{MS} \rightarrow$  pole conversion and  $\chi^2$  definition. In addition, moderate dependence exists on the rescaling parameter  $\lambda$ , associated with missing higher-order corrections. We can estimate the projected range for the  $\mathcal{O}(\alpha_s^3)$  value of  $m_c(m_c)$  by taking the central value found from method 3 and adding in quadrature the theoretical uncertainties obtained by including  $\lambda$  dependence. This produces  $1.19_{-0.15}^{+0.08}$  GeV for the estimated  $\mathcal{O}(\alpha_s^3)$  value (as shown in line 6 of the left subfigure), where the error is computed from the 68% c.l. contour for  $\chi^2$  vs.  $\lambda$  and adding scale and  $\alpha_s$  uncertainties in quadrature.

The central  $m_c$  is consistent with the PDG value of  $1.275 \pm 0.025$  GeV within the errors. A tendency of the fits to undershoot the PDG value may be attributable to the missing  $\mathcal{O}(\alpha_s^3)$  contribution [3]. The results of our fit are compatible with  $m_c(m_c)$  determined from a fit in the fixed-flavor number (FFN) scheme [3], cf. lines 5 and 7 in the left Fig. 1. However, our PDF error of about 0.15 GeV is about twice as large as that quoted in the FFN study. The reason is that in the FFN analysis the 68% c.l. PDF uncertainty is defined to correspond to  $\Delta\chi^2 = 1$  in the total  $\chi^2$ , and hence is smaller than the uncertainty according to the CT10 tolerance criterion. In our analysis, we observe that the  $\chi^2$  dependence on  $m_c(m_c)$  is not compatible with the ideal quadratic dependence required to justify the  $\Delta\chi^2 = 1$  definition for the  $1\sigma$  error. The actual  $\chi^2$  dependence is wider than the quadratic one and asymmetric, hence the  $1\sigma$  error needs to be increased by a factor of 2-3 compared to its  $\Delta\chi^2 = 1$  definition to describe the observed probability distribution. Besides this difference in the PDF uncertainty, the results for  $m_c(m_c)$  from the S-ACOT- $\chi$  and FFN fits are in agreement.

Variations in  $m_c(m_c)$  impact electroweak cross sections at the Large Hadron Collider. A plot of NNLO cross sections for Higgs and  $Z^0$  bosons production is shown at 8 TeV for  $m_c(m_c)$  ranging from 1 to 1.36 GeV and  $\lambda = \{0, 0.02, 0.05, 0.1, 0.15, 0.2\}$ . Darker color corresponds to larger mass values for a fixed  $\lambda$ . To access only the uncertainty due to the form of the rescaling variable we fix  $m_c(m_c) = 1.28$  GeV (close to the world average) and evaluate the cross sections by exploring five  $\lambda$  values (black boxes, with the size of the box increasing with  $\lambda$ ). Theoretical predictions are better clustered in this case. The empty triangle and ellipse indicate central prediction and 90% C.L. interval based on CT10 NNLO respectively. The uncertainty of LHC cross sections due to  $m_c(m_c)$  is comparable to the experimental PDF uncertainty and in principle should be included independently from the latter.

This work was supported by the U.S. DOE Early Career Research Award DE-SC0003870 and by Lightner-Sams Foundation.

## References

- [1] A. Martin et al., Eur.Phys.J. C70 (2010) 51, 1007.2624.

- [2] H1 Collaboration, ZEUS Collaboration, H. Abramowicz et al., (2012), 1211.1182.
- [3] S. Alekhin et al., (2012), 1212.2355.
- [4] W.-K. Tung, et al., JHEP **0702** (2007) 053 [hep-ph/0611254].
- [5] J. Sanchez Guillen et al., Nucl.Phys. B353 (1991) 337.
- [6] W. van Neerven and E. Zijlstra, Phys.Lett. B272 (1991) 127.
- [7] E. Zijlstra and W. van Neerven, Phys.Lett. B273 (1991) 476.
- [8] E. Laenen et al., Nucl.Phys. B392 (1993) 162.
- [9] S. Riemersma, J. Smith and W. van Neerven, Phys.Lett. B347 (1995) 143, hep-ph/9411431.
- [10] B. Harris and J. Smith, Nucl.Phys. B452 (1995) 109, hep-ph/9503484.
- [11] S. Moch, J. Vermaseren and A. Vogt, Phys.Lett. B606 (2005) 123, hep-ph/0411112.
- [12] J. Vermaseren, A. Vogt and S. Moch, Nucl.Phys. B724 (2005) 3, hep-ph/0504242.
- [13] J. Blumlein, A. De Freitas, W.L. van Neerven, S. Klein, Nucl.Phys. B755 (2006) 272; I. Bierenbaum, J. Blumlein, S. Klein, Nucl.Phys. B820 (2009) 417; J. Ablinger et al., Nucl.Phys. B844 (2011) 26; B864 (2012) 52; arXiv:1212.5950; J. Blumlein et al., Nucl.Phys. B866 (2013) 196.
- [14] H1 and ZEUS Collaboration, F. Aaron et al., JHEP 1001 (2010) 109, 0911.0884.
- [15] J. Gao, M. Guzzi and P.M. Nadolsky, (2013), 1304.3494.
- [16] M. Aivazis et al., Phys.Rev. D50 (1994) 3102; M. Kramer, I. F. I. Olness and D. E. Soper, Phys. Rev. D **62** (2000) 096007; W.-K. Tung, S. Kretzer and C. Schmidt, J.Phys. G28 (2002) 983.
- [17] M. Guzzi et al., Phys.Rev. D86 (2012) 053005, 1108.5112.
- [18] J. C. Collins, Phys. Rev. D **58** (1998) 094002.
- [19] M. Buza et al., Eur.Phys.J. C1 (1998) 301, hep-ph/9612398.
- [20] K. Chetyrkin, J.H. Kuhn and M. Steinhauser, Comput.Phys.Commun. 133 (2000) 43.
- [21] S. Alekhin and S. Moch, Phys.Lett. B699 (2011) 345, 1011.5790.
- [22] A. Chuvakin, J. Smith and W. van Neerven, Phys.Rev. D61 (2000) 096004, hep-ph/9910250.
- [23] R. Thorne and R. Roberts, Phys.Lett. B421 (1998) 303, hep-ph/9711223.
- [24] R. Thorne and R. Roberts, Phys.Rev. D57 (1998) 6871, hep-ph/9709442.
- [25] R. Thorne, Phys.Rev. D73 (2006) 054019, hep-ph/0601245.
- [26] S. Forte et al., Nucl.Phys. B834 (2010) 116, 1001.2312.
- [27] P.M. Nadolsky and W.-K. Tung, Phys.Rev. D79 (2009) 113014, 0903.2667.
- [28] J. Gao et al, (2013), 1302.6246.
- [29] H.-L. Lai et al, Phys.Rev. D82 (2010) 074024, 1007.2241.